

THE SPACE ENVIRONMENT GONIOMETER. T. J. Warren¹, I. R. Thomas¹ and N. Bowles¹, ¹Atmospheric, Oceanic and Planetary Physics, University of Oxford, Department of Physics, Clarendon Laboratory, Parks Road, Oxford, OX1 3PU, United Kingdom, (warren@atm.ox.ac.uk, thomas@atm.ox.ac.uk, bowles@atm.ox.ac.uk).

Introduction: This paper describes work currently under way in the sub-department of Atmospheric, Oceanic and Planetary Physics (AOPP) Dept. of Physics, University of Oxford to develop a ‘Space Environment Goniometer’ (SEG). The SEG is designed to support thermal infrared remote sensing measurements of airless bodies in the Solar System. In particular, it will be used to support measurements currently being made by the Diviner Lunar Radiometer (‘Diviner’), a nine-channel mapping radiometer currently in orbit around the Moon as part of NASA’s Lunar Reconnaissance Orbiter mission. The Diviner channels range from the visible to the far infrared (>400 μm) [1,2], with three channels centred on the mid-infrared (8 μm).

Typically, 3D thermal physical models of the lunar surface, which attempt to reproduce the brightness temperatures measured by Diviner [e.g. 3,4], assume infrared radiation is scattered isotropically from the lunar surface. Although generally the models are in very good agreement with the measured brightness temperatures, there are some discrepancies in shadowed regions of polar craters. In these regions the models appear to under estimate the temperature by roughly 15K [4] and one possibility is that the scattering properties of the regolith in the mid-infrared are incorrectly estimated in the models. Although significant progress is being made in determining the scattering properties of the lunar soil in the visible and near-infrared [e.g. 5,6], there is still limited or no data available on the scattering properties in the thermal or far infrared.

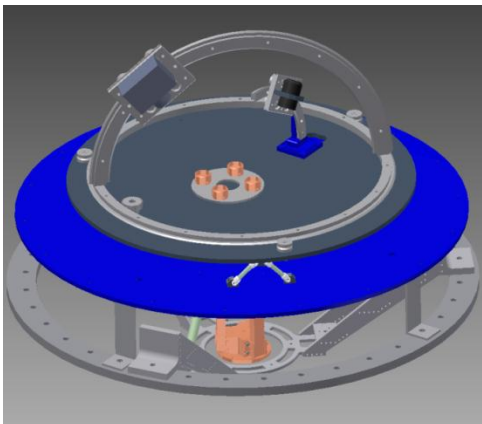


Figure 1: CAD model of the internal goniometer setup.

To fill this gap, we are developing an automated, vacuum compatible goniometer system capable of

making measurements under simulated lunar thermal conditions in the laboratory at the same wavelengths as Diviner. Once operational the goniometer will be able to measure full bidirectional reflectance distribution functions (BRDF) of lunar analogue minerals and Apollo samples. This will then allow photometric parameters [e.g. 8] to be fitted to the measurements, creating a new library of BRDF measurements directly comparable to the Diviner dataset.



Figure 2: Photograph of the goniometer currently setup on an optical bench.

Goniometer: Detailed design and construction work for the goniometer has been completed and the goniometer (Figure 1 and 2) is presently being calibrated using a certified spectralon target in the visible and near infrared for reflectance measurements. Once calibrated, the goniometer will make measurements of lunar analogue samples on an optical bench in air in the visible and near infrared. This will then allow a comparison to be made with measurements from similar goniometer systems [e.g 5,6,7]. In the future the goniometer will make measurements in the thermal and far infrared surrounded by a cold shield (< 150K) (Figure 4) inside a vacuum chamber (< 10⁻³ mbar) (Figure 5). The physical design of the goniometer is described below:

Light Source: For reflectance only measurements the goniometer currently uses a high temperature 45W quartz halogen bulb and reflector to provide a well-controlled light source. The light source is chopped and coupled down an optical fibre light guide. The output beam from the optical fibre is then collimated onto the sample.

For combined emission and reflectance measurements the light source will not be coupled down an optical fibre, but will instead be collimated directly onto the sample. In the future the light source will be upgraded to a solar-like lamp to accurately simulate the environment on the near lunar-surface.

Radiometer: The radiometer will be based on a high performance pyro-electric detector (Infratec LIE-312F [9]) with a reference chopper for emission measurements and views of a calibrated blackbody target. Wavelength selection will be provided by spare Diviner filters [2]. In the future the system will be coupled to a FTIR spectrometer to allow full spectro-goniometric measurement to be made.

Mechanical Components: Two stepper motors are used to control the position of the radiometer's azimuthal and emission angles, while another stepper motor controls the position of the light source (i.e. incidence angle). The incident angle can be varied between 0-74°, emission angle from 0-84° and the azimuth angle from 0-180°. A further stepper motor is used to control the sample changer, which can hold up to four samples, one of which is a calibrated blackbody target. A PC with Labview™ software will automate the measurement process. The minimum angular accuracy required for the goniometer to resolve the features in Figure 3 is 0.5°. The goniometer has been designed to have an angular accuracy of ~0.1°.

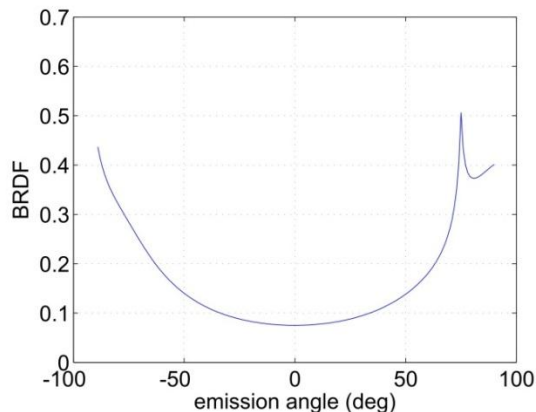


Figure 3: Calculated bidirectional reflectance data using a Hapke model at $i=60^\circ$ using Hapke parameter values fitted to BRDF measurements of Apollo samples in the near infrared in Foote et al [3].

Cold Shield and Vacuum Chamber: To reduce background thermal infrared radiation, the goniometer must be surrounded by a cold shield (<150K). To cool the cold shield to such low temperatures and prevent permafrost from condensing on the cold shield, the whole system must be enclosed in a (<10⁻³ mbar) vacuum chamber (Figure 5). The cold shield is made from 5mm aluminum alloy, and has a diameter of 0.8m and height of 0.5m. Thermal models have shown this will cool uniformly, with any temperature gradient between top and bottom <4K (Figure 4). Critical components will also be coated in high-emissivity paint (e.g. NEXTEL Black velvet) to prevent stray light reflections from affecting the measurements.

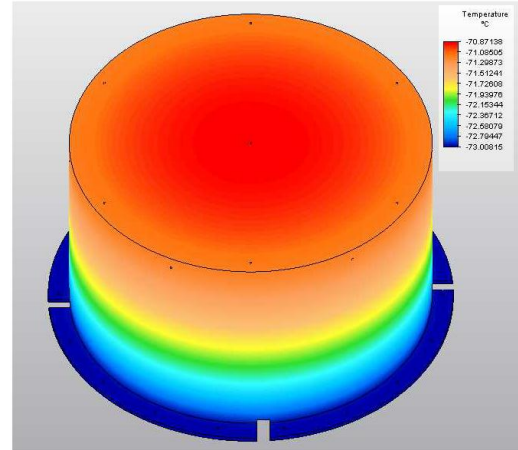


Figure 4: A thermal model of the cold shield.



Figure 5: Vacuum chamber that will enclose the goniometer and cold shield.

References: [1] Thomas I. R. et al. (2012) LPSC XXXXIII abstract #2637; [2] Paige D. A. et al. (2009) The Diviner Lunar Radiometer Experiment, Space Sci. Rev.150, 125-160; [3] Paige D. A. et al. (2010), Diviner Lunar radiometer Observations of Cold Traps in the Moon's South Polar Region, Science, 330, 479; [4] Vasavada A.R. et al., Near-Surface Temperatures on Mercury and the Moon and the Stability of Polar Ice Deposits, Icarus, 141, 179 (1999). [5] Foote, E. J. (2012) LPSC XXXXIII abstract #2357; [6] Foote, E. J. (2009) LPSC XXXX abstract #2500; [7] Shepard, M. K. (2001) LPSC XXXII abstract #1015; [8] Hapke, B. (1993) Theory of Reflectance and Emittance Spectroscopy, Cambridge Univ. Press; [9] InfraTec Ltd. (2012) LIE-312f datasheet, retrieved from: <http://www.infratec-infrared.com/Data/LIE-312f.pdf>.